ACS APPLIED MATERIALS & INTERFACES

Research Article

www.acsami.org

Advanced Photoemission Spectroscopy Investigations Correlated with DFT Calculations on the Self-Assembly of 2D Metal Organic Frameworks Nano Thin Films

Radwan Elzein,[†] Chun-Min Chang,[‡,§] Inna Ponomareva,[‡] Wen-Yang Gao,[∥] Shengqian Ma,[∥] and Rudy Schlaf*[,†]

[†]Department of Electrical Engineering, University of South Florida, Tampa, Florida 33620, United States

[‡]Department of Physics, University of South Florida, Tampa, Florida 33620, United States

[§]Institute for Cyber-Enabled Research, Michigan State University, East Lansing, Michigan 48824, United States

[∥]Department of Chemistry, University of South Florida, Tampa, Florida 33620, United States

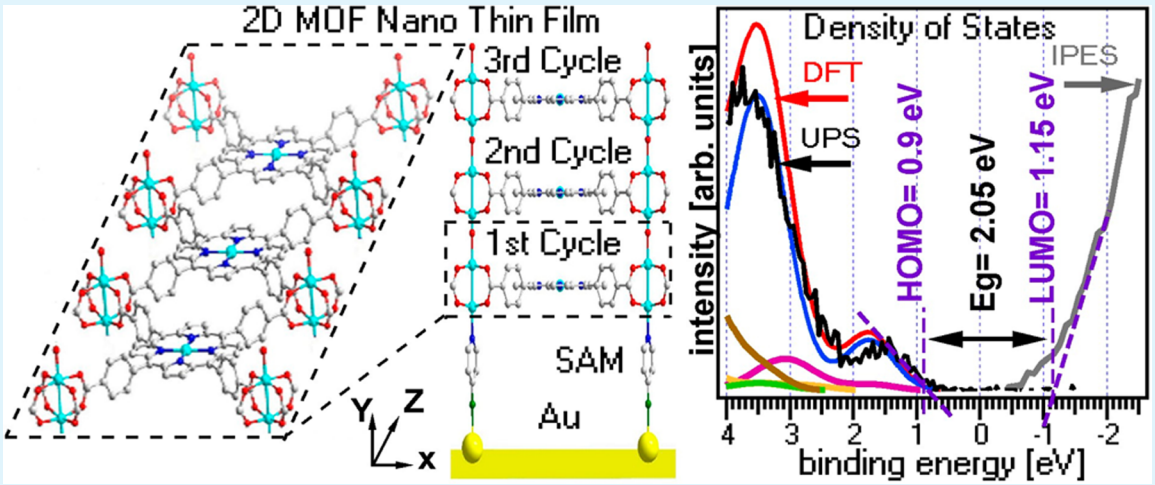

ABSTRACT: Metal−organic frameworks (MOFs) deposited from solution have the potential to form 2-dimensional supramolecular thin films suitable for molecular electronic applications. However, the main challenges lie in achieving selective attachment to the substrate surface, and the integration of organic conductive ligands into the MOF structure to achieve conductivity. The presented results demonstrate that photoemission spectroscopy combined with preparation in a system-attached glovebox can be used to characterize the electronic structure of such systems. The presented results demonstrate that porphyrin-based 2D MOF structures can be produced and that they exhibit similar electronic structure to that of corresponding conventional porphyrin thin films. Porphyrin MOF multilayer thin films were grown on Au substrates prefunctionalized with 4-mercaptopyridine (MP) via incubation in a glovebox, which was connected to an ultrahigh vacuum system outfitted with photoelectron spectroscopy. The thin film growth process was carried out in several sequential steps. In between individual steps the surface was characterized by photoemission spectroscopy to determine the valence bands and evaluate the growth mode of the film. A comprehensive evaluation of X-ray photoemission spectroscopy (XPS), ultraviolet photoelectron spectroscopy (UPS), and inverse photoemission spectroscopy (IPES) data was performed and correlated with density functional theory (DFT) calculations of the density of states (DOS) of the films involved to yield the molecular-level insights into the growth and the electronic properties of MOF-based 2D thin films.

KEYWORDS: *metal−organic frameworks, supramolecular self-assembly, 2D thin films, surface science, density of states, DFT calculations, photoemission spectroscopy*

INTRODUCTION

The past two decades have witnessed a growing interest in the area of metal−organic frameworks (MOFs), an advanced class of functional porous materials that adopts concepts from crystal engineering to self-assembled highly ordered crystalline porous materials.[1] MOFs are highly attractive to both academic and industrial communities due to their potential applications in heterogeneous catalysis,[2] gas storage,[3] gas separation,[4] drug delivery,[5] sensing,[6] or storage devices.[7] As crystalline porous coordination polymers, MOFs are constructed by connecting

Received: August 17, 2016
Accepted: October 21, 2016
Published: October 21, 2016

DOI: 10.1021/acsami.6b10340
ACS Appl. Mater. Interfaces 2016, 8, 31403−31412

metal ions or clusters with organic based ligands. This results in porous crystalline nanoscale frameworks composed of a variety of molecular compounds containing highly tunable empty space for guest molecule adsorption. Meanwhile, this also makes these materials interesting for controlled mass transfer and opens up the prospect of creating tailor designed materials with both electronic and ionic conductivity.

In particular, the self-assembly of conductive MOF structures on wafer-type supports and the investigation of their performance in device structures are of great interest for next-generation electronic device development. Such devices can be manufactured through a combination of standard lithographic techniques and molecular self-assembly of embedded MOF structures. The resultant materials integrating ionic and electronic conductivity in one single structure would exhibit promising applications in energy storage, fuel cells, and other areas. Probably the prime examples are memristive[8,7] circuit elements as demonstrated by Hewlett-Packard,[9] which demonstrate the high significance of materials with combined electronic and ionic conductivity for future technological applications. Memristors enable a remarkably simple (compared to transistor/capacitor based classic static or dynamic random access memory(RAM)) design of memory elements, which only need two terminals for read and write operations, while being able to store the information for long times without power.

The well-developed crystal engineering strategy enables us to custom design MOFs structures via the judicious selection of the metal ions and organic linkers, which also suggests the self-assembly of MOF-based device structures with electronic conductivity is viable. Among a variety of organic linkers used to fabricate nano thin films, porphyrin ligand, because of their versatility and functionality, present tremendous potential when combined with suitably chosen active SBUs. However, when applying MOF or related coordination materials on nanoelectronic devices, the main challenges to be addressed lie in controlling the size of objects at the nanoscale and aligning such objects on surface of various substances in certain desired ways without losing their original electronic properties.

In essence, π-stacked conjugated molecular structures need to be achieved in such materials. This was shown recently by Narayan et al.[10] who synthesized a conducting porous framework based on columnar stacks of TTFTB (tetrathiafulvalene tetrabenzoate). Recent research on covalent organic frameworks (COFs) has shown that conductive molecular materials like porphyrins and phthalocyanines can be used for the formation of porous structures with charge transport capabilities.[11,12] This suggests that these molecular building blocks should be employable for conductive MOF structures.

The tailor design of conductive MOF structures makes it necessary that the electronic structure can be measured to provide feedback for the design process. The presented research demonstrates that photoemission spectroscopy in combination with clean structural synthesis in a vacuum system attached glovebox can be used for the characterization of the frontier orbital structure of self-assembled MOF films. This research is based on an established track record of this measurement technique for the characterization of the electronic structure of interfaces composed of conductive small molecular as well as polymeric materials.

In essence, the photoemission spectroscopy results of both UPS and IPES measurements yield the density of states of the highest occupied molecular orbitals (HOMO), and lowest unoccupied molecular orbitals (LUMO), respectively, relative to the Fermi level. Since this measurement occurs in ultrahigh vacuum and also is very surface sensitive (only the top 5 nm are "seen") the investigated samples need to be prepared in vacuum or in the inert environment of a vacuum-attached glovebox. Such measurements were successfully demonstrated in the past for a variety of molecular materials such as conductive polymers, small molecular electroluminescent materials, self-assembled monolayers, or ribonucleic acids.

In this work, the application of this technique to self-assembled conductive MOF structures is demonstrated. Self-assembled MOF thin films were grown in several steps, while characterizing the electronic structure depending on the layer thickness. In these experiments, MOF thin films composed of TCPP linkers and dicopper paddlewheel secondary building blocks (SBU) were self-assembled on top of SAM-terminated (MP) Au substrates. The TCPP molecule is a prototypical linker-molecule candidate for conductive MOF structures, and well-suited for the presented measurements since similar measurements were already demonstrated successfully on evaporated porphyrin thin films.[13−17] The molecule MP was chosen as SAM substrate for the structure since it is capable of coordinating to the copper paddlewheels from axial positions while facilitating charge transport. These experiments were accompanied by computational DFT calculations on the DOS of the prepared MOF structures. These calculations showed strong agreement and allowed the interpretation of the photoemission data.

EXPERIMENTAL SECTION

Materials: MOF Materials: MOF Synthesis. $Cu(NO_3)_2$ and TCPP (5,10,15,20-tetrakis(4-carboxyphenyl) porphyrin); 4-mercaptopyridine (96%), as well as anhydrous ethanol were purchased from Fisher Scientific. The *N*,*N*-dimethylformamide (DMF), (ACS, 99.8+%) was obtained from Alfa Aesar, and the thin film Au (100 nm Au deposited on a 20 nm Ti adhesion layer on glass slides) substrates were purchased from EMF Corp. (Ithaca, NY).

Sample Preparation. All experiments were performed in a commercial multichamber system (SPECS Nano Analysis GmbH, Berlin, Germany) under ultrahigh vacuum (UHV) conditions (2×10^{-10} mbar base pressure). The system consists of a fast entry lock, transfer chamber for sputtering, and analysis chambers equipped with X-ray, ultraviolet, and inverse photoemission spectroscopy (XPS, UPS, and IPES, respectively). A homemade acrylic glovebox was attached to the load lock to enable a direct transfer of the sample from the sample preparation area into the vacuum. The glovebox was filled with 99.995% N2 and kept under slight overpressure to suppress sample contamination from the ambient environment during sample preparation.

The thin film Au (100 nm thick) substrates were cut into 1×1 cm^2 pieces and mounted on a substrate holder via screws. This allowed for direct electrical contact between the Au layer and the chamber ground to avoid charging effects. The substrates were then transferred into an UHV chamber for sputtering to clean the Au surface. A SPECS IQE 11/35 ion source with a kinetic energy of 5 keV and an emission current of 20 mA was used, and the sample sputtered for 40 min at an Ar pressure of 4 mbar.[18]

After sputtering, the clean Au substrates were characterized by the standard measurement sequence beginning with an LIXPS measurement (Mg K, 1253.6 eV, standby mode: 0.1 mA emission current), then followed by UPS (He I, 21.2182 eV), XPS (Mg K, 1253.6 eV, 20 mA emission current), and finally an IPES measurement (electron gun, Kimball ELG-2/EGPS-1022, and a Geiger counter with an energy resolution of about 0.43 eV).

The deposition experiments started by loading an Au substrate into the glovebox for the growth of the SAM via incubation. The sample was placed into the bottom of a vial containing the SAM solution (1 mM SAM solution of 4-mecaptopyridine in ethanol stirred at 80 °C for 24 h).

DOI: 10.1021/acsami.6b10340
ACS Appl. Mater. Interfaces 2016, 8, 31403−31412

Scheme 1. Schematic Depiction of the Growth Sequence: MOF Films Were Grown in Three Incubation Cycles on a MP SAM-Terminated Gold Substrate[a]

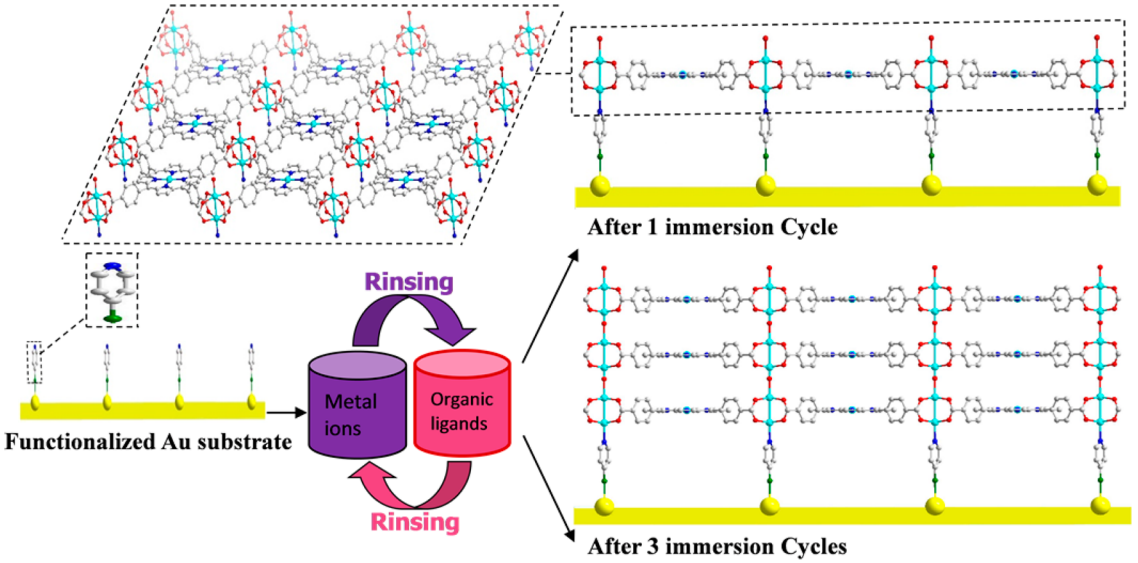

[a]First, the sample was incubated in the metal ion solution ($Cu(NO_3)_2$), followed by immersion into the organic ligand solution (TCPP). Each incubation step was completed by rinsing the sample in DMF and deionized water. Color assignment: carbon, gray; oxygen, red; sulfur, green; nitrogen, blue; and copper, cyan.

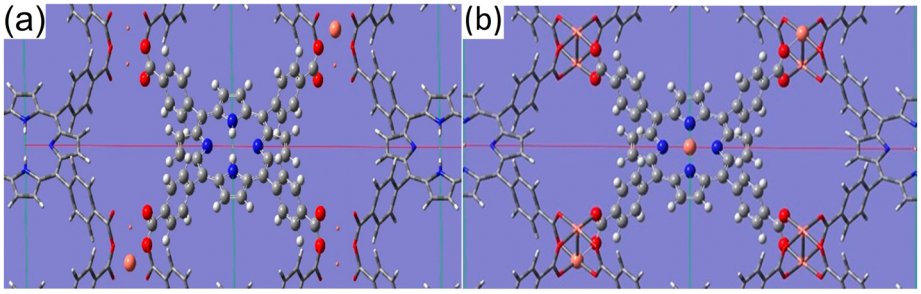

Figure 1. Computed structures of MOF molecules connected to Cu paddle wheels. (a) Free base TCPP and (b) metalated CuTCPP.

The vial was sealed and placed in the glovebox for 24 h at 40 °C. After cooling the sample to room temperature, it was removed and then rinsed gently with ethanol, deionized water, and dried with a stream of 99.995% N_2.

In the first MOF experiment (A), the Au functionalized substrate was alternately immersed into the metal ion solution (13.329 mM $Cu(NO_3)_2$ solution in DMF stirred on a hot plate at 80 °C for 24 h) for 12 h followed by an immersion step in the organic ligand solution (1.2645 mM TCPP solution in DMF stirred on a hot plate at 80 °C for 24 h) for an additional 12 h, three sequential incubation cycles were performed in the glovebox at a temperature of 40 °C. In between each immersion step, the substrate was rinsed with fresh DMF and deionized water to remove excessive unbound molecules from the surface,[19] and dried in a stream of 99.995% N_2 as depicted in (Schematic 1), which shows the expected crystal structure.[20] Following each individual immersion cycle, the surface was characterized with the above LIXPS/UPS/XPS sequence.

In a control experiment (B), fresh TCPP and $Cu(NO_3)_2$ solutions were mixed together in a vial following the same concentrations and conditions reported in the main experiment (A). An identical Au functionalized surface was immersed into a vial containing the mixed solution for three incubation cycles in the glovebox each for 24 h at 40 °C (identical conditions as in experiment A). After each complete incubation cycle, the substrate was rinsed with DMF and deionized water, and then dried with 99.995% N_2. This was followed by transfer into the attached vacuum system and PES characterization.

In the second control experiment (C), the Au functionalized surface was immersed in the TCCP solution (same concentration and experimental conditions as were used in experiment (A)), but the immersion in the $Cu(NO_3)_2$ solution was omitted. After the experiment, the sample was inserted into the vacuum system and then characterized by PES.

Computational Method for DFT Calculations on the Electronic Structure. The molecular modeling software Gaussian09 was used to perform all-electron DFT calculations on the metalated and free base TCPP molecules connected to copper paddle wheels.[20] The computed structure of TCPP can be seen from Figure 1a and that of CuTCPP is shown in Figure 1b.

The Gaussian basis set 6-311G** and DFT exchange correlation functional B3LYP with 2-dimensional periodic boundary condition were employed. The ground-state geometries of both MOF structures were fully optimized in vacuum, then the electronic structure and the energy levels were calculated. By considering possible deformation and thermal effects in the system, the theoretical DOS spectra are plotted by Gaussian broadening of the intensity around each energy eigenvalue. The results are compared with experimental UV photoelectron spectra in the Discussion section.

RESULTS

The standard LIXPS-UPS-XPS measurement sequence was carried out after each sample preparation step. Figure 2 shows the evolution of the C 1s, N 1s, O 1s, S 2p, Cu 2p, and Au 4f core level emission lines throughout the three experiments A, B, and C.

DOI: 10.1021/acsami.6b10340
ACS Appl. Mater. Interfaces 2016, 8, 31403−31412

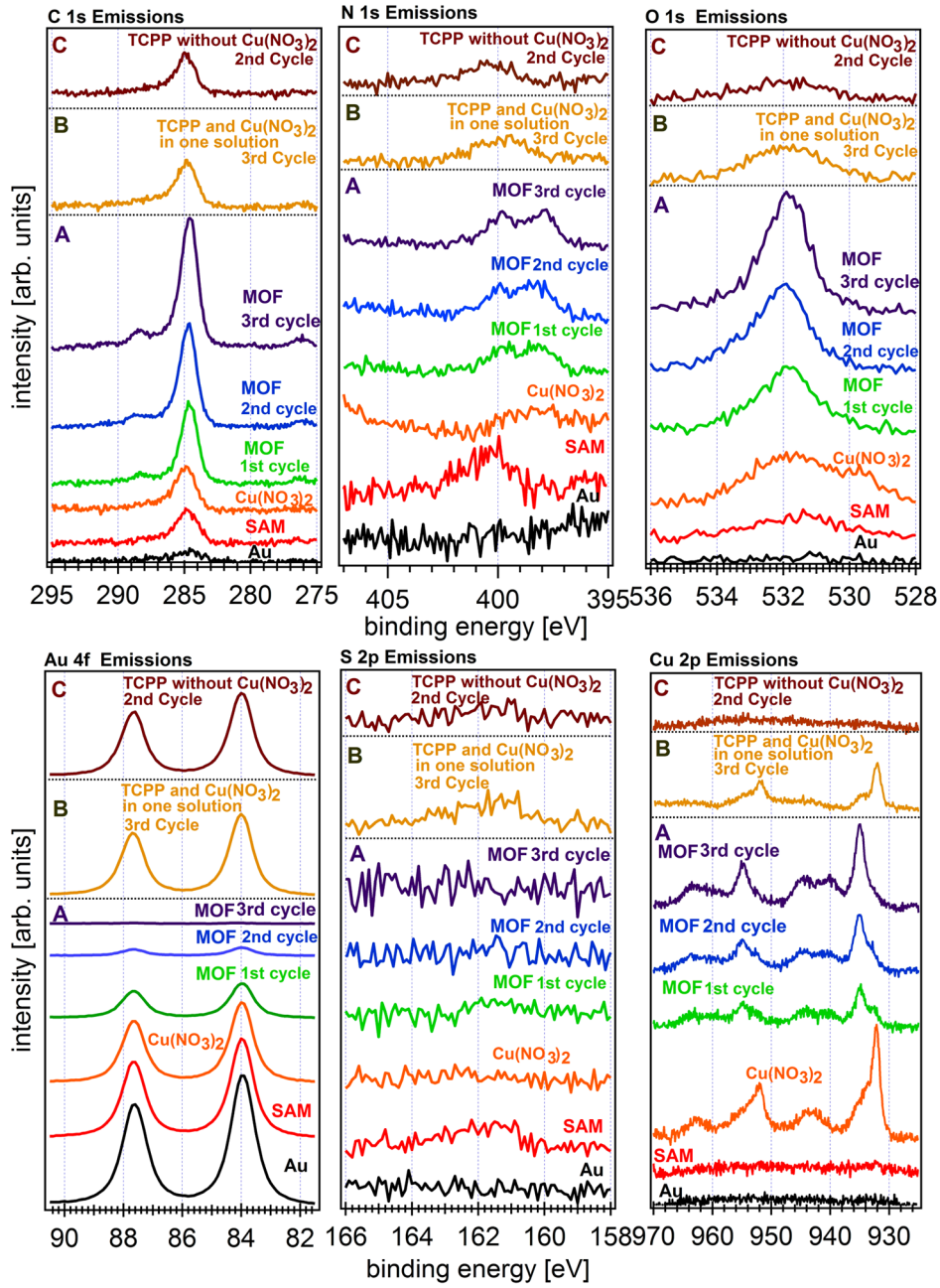

Figure 2. C 1s, N 1s, O 1s, Au 4f, S 2p, and Cu 2p core level XPS spectra measured before and after step-by-step incubation on the functionalized Au substrate (A) in the $Cu(NO_3)_2$ solution, then in the TCPP solution for three cycles sequentially, (B) in both the $Cu(NO_3)_2$ and the TCPP solution for three cycles sequentially, and (C) only in a TCPP solution for two cycles.

The bottom spectra correspond to the sputtered Au substrate as measured for experiment A. Experiments B, and C yielded similar spectra. The following spectra correspond to the incubations steps performed on each of the samples. The spectra measured for the clean substrate shows only weak O 1s and C 1s peak emissions at around 531 and 284.8 eV respectively. These peaks are related to residual contamination from the sample holder assembly.

In the first experiment (A), the Au 4f signals were attenuated gradually after each incubation cycle, the third cycle has negligible intensity compared to the first cycle which clearly indicates the surface has a substantial MOF growth with increasing thickness. The intensities before and after incubations allowed for an estimation of deposited layer thickness using the Lambert–Beer law with a mean free path of 0.18 and 33 Å for the emitted electrons of Au 4f through SAM,[21,22] and porphyrin derivatives,[23,24] respectively. The approximate thickness of the SAM is 0.45 nm, which is commensurate with the length of the molecule assuming it is aligned vertically on top of the Au surface. The individual layer thicknesses of the MOF first cycle, MOF second cycle, MOF third cycle, are 39.94, 77.13, and 112.7 Å, respectively. The Au 4f emission features of the second (B) and third (C) experiments only show attenuation consistent to the SAM incubation cycle, but there is no further attenuation after incubation in the MOF solutions. This indicates that the MOF only grows if the SBU is present on the surface before the linker is offered.

The S 2p emission feature of the SAM has a binding energy of about 161 eV consistent with S in the thiolate form bonded to an Au surface.[25] This emission feature disappeared only in the first experiment (A) during the MOF incubation cycles, while it

DOI: 10.1021/acsami.6b10340
ACS Appl. Mater. Interfaces 2016, 8, 31403–31412

remained unchanged in the control experiments. This further supports the conclusion that the MOF film only grows if Cu $(NO_3)_2$ was deposited prior to incubation in TCPP. A similar behavior is seen in all other MOF overlayer related emissions. MOF-related emissions occur only in experiment A, while experiments B and C do not show much change after the SAM has grown.

The aromatic hydrocarbon related C 1s emission features of both SAM and TCPP multilayers produce a peak at about 285 eV. The distinguishing element in the C 1s spectra of the MOF layer has a smaller emission at about 288 eV, which is related to C—O bonds, which are found in the COOH groups of the MOF.[26,27] This feature only occurs in experiment (A), while the emissions seen in (B) and (C) retain their shape, intensity, and binding energy during the incubation steps. This support that no film grew on top of the SAM layer.

The O 1s emission featured shows a similar behavior. There is a small O 1s emission feature present after the SAM growth step. This emission line is related to the residual surface contamination of surrounding areas on the substrate holder.[28] In experiment (A), this emission is attenuated at the expense of a strong new peak that is related to the COOH groups present in the MOF film.[29] Control experiment (B) shows a change in the O 1s spectrum due a small amount of deposited $Cu(NO_3)_2$ indicating that some molecules deposited on the surface during the incubation step. Experiment (C) shows again no change relative to the initial SAM layer, indicating that no film deposition. This clearly shows that Cu $(NO_3)_2$ needs to be present on the surface before incubation in TCPP if a thin film is to be grown.

The Cu 2p emission from the $Cu(NO_3)_2$ (orange spectrum) shows only contributions of Cu(I) with a binding energy of 932.4 eV. However, once the TCPP was added onto the surface, the Cu 2p emission (purple spectrum) revealed Cu(II) characteristic at 936.1 eV and additional satellite peaks at 940 and 944.3 eV assuming a Cu paddle wheel SBU was assembled by self-organization in situ by the presence of TCPP. This is also supported by the particular structure of the observed emissions, which agree well with the data published by other groups.[30,31] In addition, the binding energy of the spectra changes significantly once the MOF film forms. This is seen in the sequence of spectra of experiment (A) as the MOF film grows in thickness. The initial spectrum measured after the $Cu(NO_3)_2$ deposition step is gradually attenuated, while a spectrum with peaks shifted by about 3 eV to higher binding energy arises. This indicates a charge transfer from the $Cu(NO_3)_2$ building blocks to the TCPP spacers as the MOF forms.

The analysis of the N 1s spectra sequence is consistent with the Cu 2p series. The initial N 1s spectrum (red) of the SAM shows a broad peak at about 400.1 eV, which confirms the deposition of MP on the Au surface. The N 1s spectra measured during the growth of the MOF film (green spectrum) during experiment (A) exhibit distinctly different emission features that are attributed to a molecule containing pyrolic (—NH—) and iminic (—N═) nitrogen species. These are strong indicators that an interaction between Cu atoms and TCPP molecules took place. These emission lines are located at 397.9 and 399.8 eV, respectively, which are in close agreement with other experiments found in the literature.[32−40]

The shift of Cu 2p to higher binding energies and the N 1s to lower binding energies indicate that electrons were donated from the copper atoms to the TCPP molecules, as electron loss usually results in higher binding energies.[18]

In summary, the XPS data clearly show that a layered self-assembly process of an MOF structure occurs between the $Cu(NO_3)_2$ and TCPP molecular units when $Cu(NO_3)_2$ is deposited on the surface before the TCPP incubation steps. When $Cu(NO_3)_2$ and TCPP are directly mixed in solution, this process does not occur, possibly due to the formation of 3D MOF structures in solution which do not deposit on the presented SAM surfaces.

UPS and LIXPS Measurements. Prior to each XPS measurement sequence, the samples were characterized with UPS and LIXPS. LIXPS uses the XPS, an X-ray gun in its standby setting, i.e., uses a very low photon density. This low density is still enough to perform a successful measurement of the secondary edge, i.e., the work function can be detected. This approach allows the detection of charging artifacts that often occur during UPS measurements due to the relatively high photon density of UV sources. Especially on organic materials this can be an issue due to the often low conductivity of these materials, which prevents the effective replenishment of photo extracted electrons. This causes charging, which manifests itself in peak shifts. LIXPS is much less affected by charging phenomena, i.e., comparing UPS, and LIXPS work function measurements reveal the onset of charging artifacts in UPS measurements.[41,42]

The UP- and LIXP-spectra measured in conjunction with the XPS spectra of Figure 2 are shown in Figure 3. The center graph shows the full UP-spectra measured after each experimental step. The left graph shows the corresponding LIXPSa and LIXPSb (dashed lines) spectra as measured before and after the UPS measurements, respectively. The right part shows the valence bands/HOMO regions of the spectra. 0 eV represents the Fermi energy.

The secondary edge feature of the LIXP-spectra, located between 16 and 18 eV, is defined by the work function of the sample (Figure 3, left panel). Each incubation cycle produced intense spectral lines corresponding to the frontier orbital states of the deposited molecules, while strongly attenuating the Au emissions. The secondary cutoff shifted to higher binding energy after each of the incubations, indicating a decrease in the Au surface work function due to the interaction between the surface and the MOF film. The work functions were determined after each incubation step by measuring the high binding energy cutoff at the secondary edge where the spectra ends are located. This value is 15.9752 eV in case for Au. Hence, the work function can be determined by the difference between the energy of the UV photons (21.2182 eV for He I excitation energy) and the Au binding energy (black spectrum) of the secondary edge 15.9752 eV, and by adding the analyzer broadening (analyzer correction factor) of approximately 0.1 eV. Similarly, the work functions of the SAM and MOF, 4.3 and 5.16 eV, respectively, were determined from the LIXPS measurements rather than the UPS measurements to avoid any charging artifacts or photochemical surface modifications that can occur during the UPS measurement.

The valence bands and the HOMO regions after background subtraction are shown in Figure 3, right panel, the bottom (black) spectrum shows the typical emissions for a clean Au surface after in situ sputtering. After step-by-step incubations of the metal ions and the organic ligands, the Au features are attenuated and replaced by emissions related to the valence bands/HOMO levels of the SAM film (red spectrum) and the MOF film (green, blue, and purple spectra).

DOI: 10.1021/acsami.6b10340
ACS Appl. Mater. Interfaces 2016, 8, 31403−31412

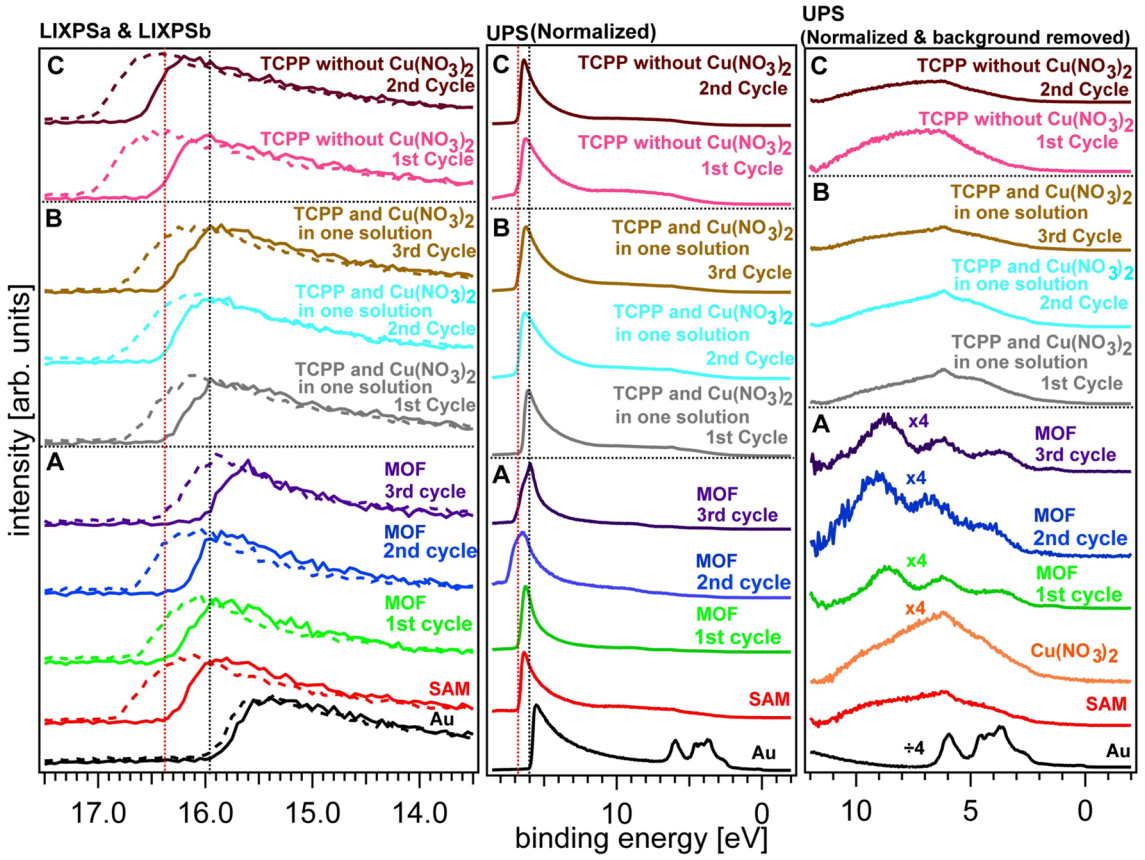

Figure 3. LIXPS and UP spectra before and after step-by-step incubation of sputter cleaned Au functionalized substrate in (A) in the metal ion $Cu(NO_3)_2$ then in the organic ligands TCPP for three cycles sequentially, (B) in both the metal ion and the organic ligand solution for three cycles sequentially, and (C) only in a TCPP solution for two cycles. Their normalized secondary edges were measured with LIXPS before (LIXPSa) and after (LIXPSb) UPS and are shown in the left panel. The complete normalized UP spectra are displayed in the middle. The right panel shows the evolution of the valence band/HOMO emission features through the deposition process.

DISCUSSION

The data show that the film only grows when the surface of the SAM substrate is "seeded" for the growth process with the $Cu(NO_3)_2$ SBUs. The second control experiment (C) showed that no significant layer growth occurs during incubation in TCPP without a prior deposition of $Cu(NO_3)_2$. This is a good indicator that a MOF structure is indeed growing. This is supported by the emergence of an additional emission at about 400 eV, which indicates the formation of bonds between the $Cu(NO_3)_2$ building blocks and the TCPP molecules. Unfortunately, a direct proof of the formed layer structure was not possible with our experimental setup. Since photoemission spectroscopy experiments with in situ preparation require the deposition of ultrathin layers to prevent charging artifacts from occurring the available sample preparation facilities are not setup for the deposition of films thick enough for XRD experiments. Hence, further experiments are needed to clarify the crystal structure directly.

The UPS valence bands spectra of the MOF films show a four-peak structure that closely resembles spectra measured recently on in-vacuum deposited Co metalloporphyrin multilayer films[13] and free base porphyrin.[14] However, the Cu 2p energy shifts to higher binding energies and the N 1s to lower binding energies suggest that the interaction between the $Cu(NO_3)_2$ building blocks and the TCPP molecules also leads to a metallization of the porphyrin molecules. This was taken into account for the DOS calculations where both free base TCPP and CuTCPP molecules connected to Cu paddlewheels were assembled into the MOF structures. The measured UPS spectrum of free base TCPP in comparison with the calculated DOS structures of both free base TCPP and CuTCPP are shown in Figures 4 and 5, respectively.

The spectrum is background subtracted, and the calculated DOS curves were shifted to match the peak positions. This was necessary since the calculation was performed on a slab of the MOF structure suspended in vacuum, while the physical film was deposited on an Au/SAM substrate, which references its electronic structure to the substrate surface via interface dipoles. The spectrum shows four emission peaks below the Fermi level.

The peaks are at 1.5, 3.75, 6.35, and 8.75 eV in both experiment (black) and computed DOS (red). These emissions can be mainly assigned to C 2p, O 1s, N 2p, Cu 2p, and H 1s orbitals. This is evident from the projected DOS curves in Figures 4 and 5, which show the individual contributions from each of the atomic species present in the prepared films. The Cu 2p emission peak has a major and broader contribution from CuTCPP molecules than TCPP molecules. Not surprisingly, this peak is also the emission feature that shows the most significant differences relative to the spectrum measured on a pure TCPP film.[15] It is denoted from various experiments found in literature that there are significant similarities between UPS spectral features of metalated and H2-porphyrin or H2 phthalocyanine thin films.[13,15] This concludes that the experimental electronic structure of the deposited MOF multilayer film Figure 4 has similar distinguished

DOI: 10.1021/acsami.6b10340
ACS Appl. Mater. Interfaces 2016, 8, 31403−31412

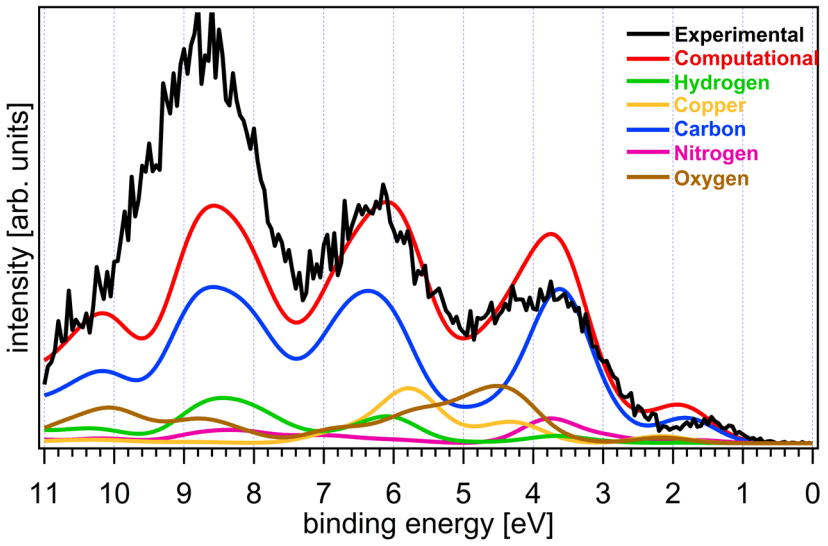

Figure 4. DOS comparison between the experimental and computational results. Four emission peaks above the Fermi level are shown in blue line from UP spectra of the MOF thin film growth consisted of $Cu(NO_3)_2$ and TCPP on top of functionalized Au substrate. The computational DOS is in red line and PDOS from each individual atomic contribution are presented with different colors.

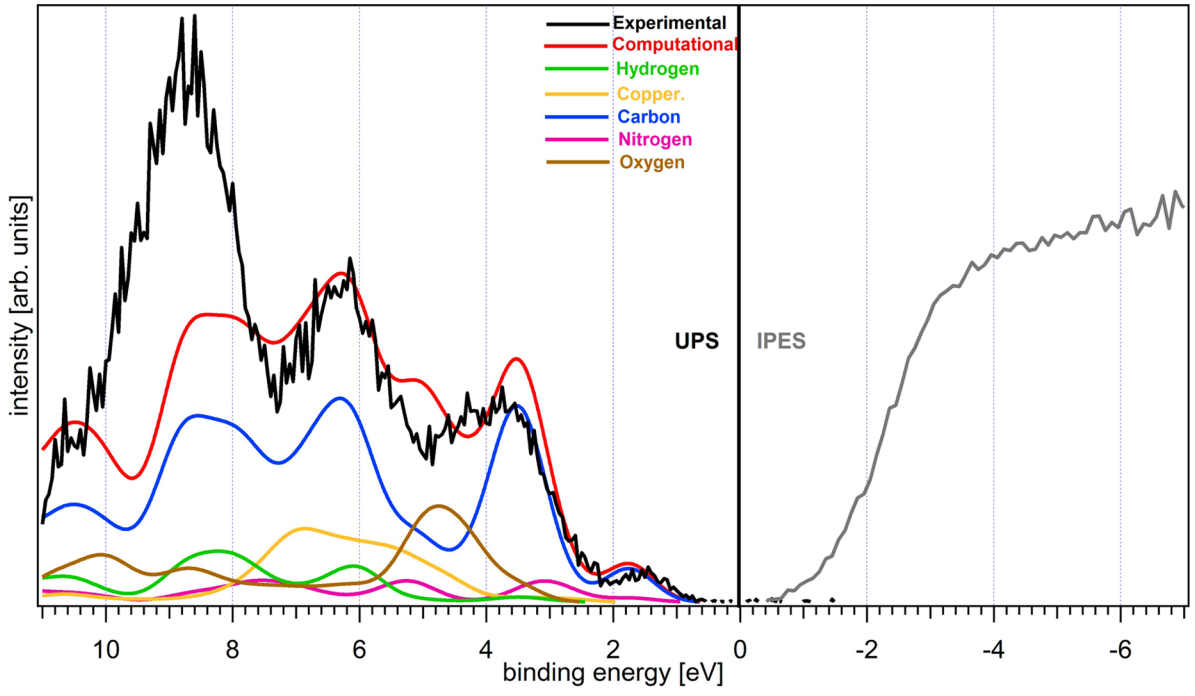

Figure 5. DOS comparison between the experimental UPS, IPES, and computational results. Four emission peaks above the Fermi level are shown in blue line from UP spectra of the MOF thin film growth consisted of $Cu(NO_3)_2$ and CuTCPP on top of functionalized Au substrate. The computational DOS is in red line and PDOS from each individual atomic contribution are presented with different colors.

spectral features compared to that of pure TPP multilayer film,[13,16] but differs from a TCPP monolayer film.[43]

In the area of the Fermi edge, the experimental spectrum of CuTCPP connected to Cu-paddlewheels (black spectrum) shows a peak of the highest occupied states around 1.5 eV which agrees with the corresponding peaks in the theoretical DOS (red spectra) of free and metalated TCPP in Figures 4 and 5, respectively.

The HOMO orbitals of CuTCPP can be seen in Figure 6a,b with spin-up and spin-down, respectively. The Lowest Unoccupied Molecular (LUMO) orbitals of CuTCPP with spin-up on the upper copper and the other is spin down on the lower copper paddle-wheel are shown in Figure 6c,d, respectively. The band gap value obtained from the DFT calculation for CuTCPP is 2.07 eV. The LUMO and HOMO of TCPP connected to copper paddle wheels can be seen as shown in Figure 6e,f, respectively. The corresponding band gap value obtained from the DFT calculation is 0.95 eV.

The onset of the first UPS peak from the MOF (CuTCPP) experimental result (black spectrum) in Figure 5 located at the lowest binding energy 0.9 eV represents the hole injection barrier Φ_h of the HOMO level at the Au functionalized surface/MOF interface, and the onset of the first IPES peak from the same experiment (gray spectrum) revealed at −1.15 eV which represents the electron injection barrier Φ_e of the LUMO level which

DOI: 10.1021/acsami.6b10340
ACS Appl. Mater. Interfaces 2016, 8, 31403−31412

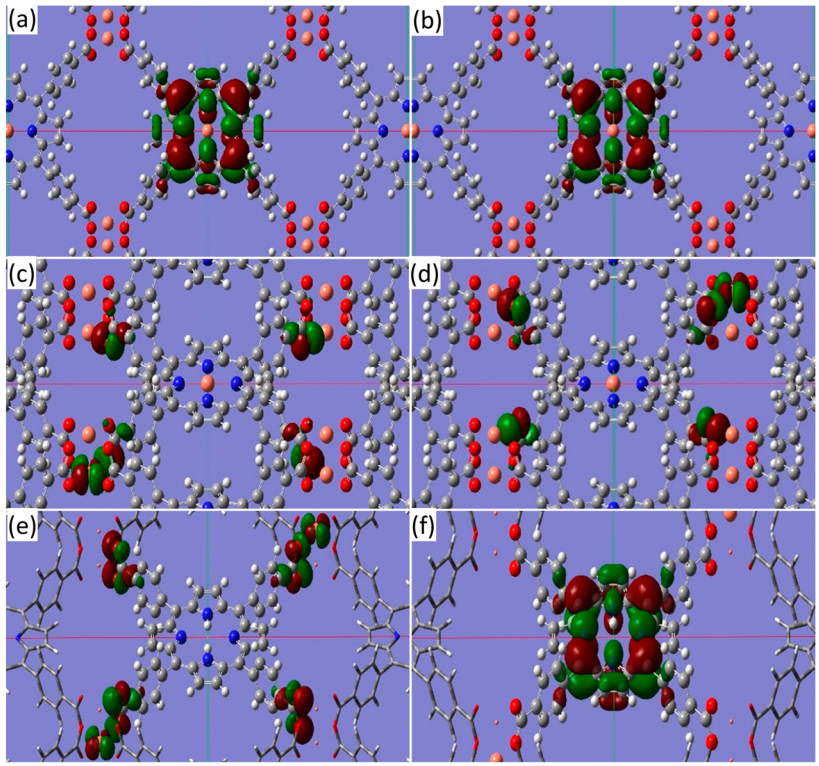

Figure 6. Computed structure of CuTCPP connected to Cu paddle wheels: (a) HOMO orbital with spin-up, (b) HOMO orbital with spin-down, (c) LUMO orbital with spin-up, and (d) LUMO orbital with spin down. Computed structure of TCPP connected to Cu paddle wheels: (e) LUMO orbital and (f) HOMO Orbital.

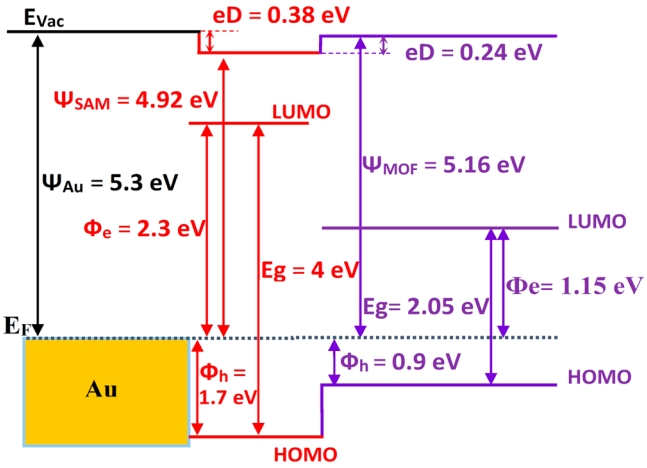

Figure 7. Electronic structure of the interface of the MOF (CuTCPP) 2D thin film grown on Au functionalized surface as determined from the UP-, IPE-, and LIXP-spectra measurements.

was shifted by −0.43 eV taking the energy resolution into account as shown in the electronic structure of Figure 7. The corresponding experimental band gap is 2.05 eV, and this agrees with the transfer gap value of 2.07 eV obtained from the full range of the computational DFT calculations of the DOS; and this also suggests that the interaction between the $Cu(NO_3)_2$ building blocks and the TCPP molecules also leads to a metallization of the porphyrin molecules. In contrast, the transfer gap values for porphyrin and its derivatives vary in the literature from 2.34 eV up to 2.9 eV.[14,17]

The ionization energy (Eion) of the MOF, found to be 6.06 eV, was determined by adding the work function of the MOF (CuTCPP) to the hole injection barrier. Although the Fermi level is close to the HOMO of the MOF and the hole injection barrier is smaller than the electron injection barrier, it is difficult to infer the conduction type due to the low carrier density in the very thin MOF film (11.27 nm), and the energy of the frontier orbitals of the MOF layered structures depends strongly on the metal work function, and the SAM. The HOMO onset of the SAM revealed at 1.7 eV which was obtained from the UPS measurement from Figure 3 (red spectrum) and the corresponding HOMO−LUMO gap is 4−4.1 eV which was adapted from the work published in reference.[44]

MOFs offered the possibility to form significant multilayer growth with high injection barriers due to the self-organization of the MOF on top of an Au functionalized surface. The bond created between the hosting functionalized substrate surface and the MOF offers a path to charge transfer due to the carrier injection barrier of 0.9 eV.

CONCLUSIONS

Self-assembly of metal organic framework was used to generate a self-organized conductive 2D MOF nano film on top of Au functionalized substrate via sequential step-by-step incubation cycles. The growth of the MOF film was determined by ultraviolet and X-ray Photoemission spectroscopy and compared to DFT calculations, and this represents a significant advance with unprecedented investigation.

The increase of the emission features of the C 1s, N 1s, O 1s, and Cu 2p and the decrease of the Au 4f and S 2p obtained through XPS measurement after sequential incubations were reliable indicators of the adsorption and the surface coverage of the MOF film on the surface of the substrate. The control experiments determined that the metal ion, $Cu(NO_3)_2$, was an essential and

DOI: 10.1021/acsami.6b10340
ACS Appl. Mater. Interfaces 2016, 8, 31403−31412

suitable SBU as a linker between SAM and the arm groups of organic ligand.

The UPS results revealed the orbitals line-up of the MOF molecules bound to the surface of the Au-functionalized surface and revealed similar emission spectral features in correlation with DFT calculations. The combined results from the first onsets of UP- and IPE-spectra revealed the band gap which strongly agrees with the value obtained from DFT calculations. The orbital line-up showed significant barriers for both hole and electron injections from the Au functionalized surface to the MOF thin film, and this property at the interface is crucial to the design and development of conductive MOF materials that can offer an important breakthrough in molecular electronic devices.

AUTHOR INFORMATION

Corresponding Author

*E-mail: schlaf@usf.edu (R.S.).

Author Contributions

The manuscript was written through contributions of all authors. All authors have given approval to the final version of the manuscript.

Notes

The authors declare no competing financial interest.

ACKNOWLEDGMENTS

R.S. gratefully acknowledges the funding from the National Science Foundation (grant# NSF DMR-1035196).

REFERENCES

(1) Li, J.-R.; Kuppler, R. J.; Zhou, H.-C. Selective Gas Adsorption and Separation in Metal-Organic Frameworks. *Chem. Soc. Rev.* **2009**, *38* (5), 1477−1504.

(2) Zou, R.-Q.; Sakurai, H.; Xu, Q. Preparation, Adsorption Properties, and Catalytic Activity of 3D Porous Metal−Organic Frameworks Composed of Cubic Building Blocks and Alkali-Metal Ions. *Angew. Chem., Int. Ed.* **2006**, *45* (16), 2542−2546.

(3) Luo, J.; Xu, H.; Liu, Y.; Zhao, Y.; Daemen, L. L.; Brown, C.; Timofeeva, T. V.; Ma, S.; Zhou, H.-C. Hydrogen Adsorption in a Highly Stable Porous Rare-Earth Metal-Organic Framework: Sorption Properties and Neutron Diffraction Studies. *J. Am. Chem. Soc.* **2008**, *130* (30), 9626−9627.

(4) Long, J. R.; Yaghi, O. M. The Pervasive Chemistry of Metal-Organic Frameworks. *Chem. Soc. Rev.* **2009**, *38* (5), 1213−1214.

(5) Horcajada, P.; Serre, C.; Vallet-Regí, M.; Sebban, M.; Taulelle, F.; Férey, G. Metal−Organic Frameworks as Efficient Materials for Drug Delivery. *Angew. Chem., Int. Ed.* **2006**, *45* (36), 5974−5978.

(6) Suh, M. P.; Cheon, Y. E.; Lee, E. Y. Syntheses and Functions of Porous Metallosupramolecular Networks. *Coord. Chem. Rev.* **2008**, *252* (8−9), 1007−1026.

(7) Yoon, S. M.; Warren, S. C.; Grzybowski, B. A. Storage of Electrical Information in Metal−Organic-Framework Memristors. *Angew. Chem., Int. Ed.* **2014**, *53* (17), 4437−4441.

(8) Chua, L. O.; Sung, M. K. Memristive Devices and Systems. *Proc. IEEE* **1976**, *64* (2), 209−223.

(9) Strukov, D. B.; Snider, G. S.; Stewart, D. R.; Williams, R. S. The Missing Memristor Found. *Nature* **2008**, *453* (7191), 80−83.

(10) Narayan, T. C.; Miyakai, T.; Seki, S.; Dincă, M. High Charge Mobility in a Tetrathiafulvalene-Based Microporous Metal−Organic Framework. *J. Am. Chem. Soc.* **2012**, *134* (31), 12932−12935.

(11) Wan, S.; Guo, J.; Kim, J.; Ihee, H.; Jiang, D. A Belt-Shaped, Blue Luminescent, and Semiconducting Covalent Organic Framework. *Angew. Chem.* **2008**, *120* (46), 8958−8962.

(12) Wan, S.; Guo, J.; Kim, J.; Ihee, H.; Jiang, D. A Photoconductive Covalent Organic Framework: Self-Condensed Arene Cubes Composed of Eclipsed 2D Polypyrene Sheets for Photocurrent Generation. *Angew. Chem., Int. Ed.* **2009**, *48* (30), 5439−5442.

(13) Lukasczyk, T.; Flechtner, K.; Merte, L. R.; Jux, N.; Maier, F.; Gottfried, J. M.; Steinrück, H.-P. Interaction of Cobalt(II) Tetraarylporphyrins with a Ag(111) Surface Studied with Photoelectron Spectroscopy. *J. Phys. Chem. C* **2007**, *111* (7), 3090−3098.

(14) Rojas, G.; Chen, X.; Bravo, C.; Kim, J.-H.; Kim, J.-S.; Xiao, J.; Dowben, P. A.; Gao, Y.; Zeng, X. C.; Choe, W.; Enders, A. Self-Assembly and Properties of Nonmetalated Tetraphenyl-Porphyrin on Metal Substrates. *J. Phys. Chem. C* **2010**, *114* (20), 9408−9415.

(15) Nardi, M. V.; Detto, F.; Aversa, L.; Verucchi, R.; Salviati, G.; Iannotta, S.; Casarin, M. Electronic Properties of CuPc and H2Pc: an Experimental and Theoretical Study. *Phys. Chem. Chem. Phys.* **2013**, *15* (31), 12864−12881.

(16) Rojas, G. Self Assembly and Interface Chemistry of Non-Metallated Tetraphenyl Porphyrin. PhD thesis, University of Nebraska—Lincoln: Lincoln, 2011.

(17) He, C.; He, Q.; Deng, C.; Shi, L.; Zhu, D.; Fu, Y.; Cao, H.; Cheng, J. Turn on Fluorescence Sensing of Vapor Phase Electron Donating Amines via Tetraphenylporphyrin or Metallophenylporphrin Doped Polyfluorene. *Chem. Commun.* **2010**, *46* (40), 7536−7538.

(18) Wolak, M. u. A.; Balaeff, A.; Gutmann, S.; Helmrich, H. J.; Vosloo, R.; Beerbom, M. M.; Wierzbinski, E.; Waldeck, D. H.; Bezer, S.; Achim, C.; Beratan, D. N.; Schlaf, R. Electronic Structure of Self-Assembled Peptide Nucleic Acid Thin Films. *J. Phys. Chem. C* **2011**, *115* (34), 17123−17135.

(19) Wolak, M. The Electronic Structure of Biomolecular Self-Assembled Monolayers. PhD thesis, University of South Florida: Tampa, 2012.

(20) Xu, G.; Yamada, T.; Otsubo, K.; Sakaida, S.; Kitagawa, H. Facile "Modular Assembly" for Fast Construction of a Highly Oriented Crystalline MOF Nanofilm. *J. Am. Chem. Soc.* **2012**, *134* (40), 16524−16527.

(21) Seah, M. P.; Briggs, D. *Practical Surf. Anal. Auger X-Ray Photoelectron Spectrosc.*; John Wiley & Sons: New York, 1990.

(22) Manolova, M.; Ivanova, V.; Kolb, D.; Boyen, H.-G.; Ziemann, P.; Büttner, M.; Romanyuk, A.; Oelhafen, P. Metal Deposition onto Thiol-Covered Gold: Platinum on a 4-Mercaptopyridine SAM. *Surf. Sci.* **2005**, *590* (2), 146−153.

(23) Boeckl, M. S.; Bramblett, A. L.; Hauch, K. D.; Sasaki, T.; Ratner, B. D.; Rogers, J. W. Self-Assembly of Tetraphenylporphyrin Monolayers on Gold Substrates. *Langmuir* **2000**, *16* (13), 5644−5653.

(24) Bramblett, A. L.; Boeckl, M. S.; Hauch, K. D.; Ratner, B. D.; Sasaki, T.; Rogers, J. W. Determination of Surface Coverage for Tetraphenylporphyrin Monolayers using Ultraviolet Visible Absorption and X-ray Photoelectron Spectroscopies. *Surf. Interface Anal.* **2002**, *33* (6), 506−515.

(25) High Resolution XPS of Organic Polymers: The Scienta ESCA300 Database Beamson, G.; Briggs, D. *J. Chem. Educ.* **1993**, *70* (1), A25.

(26) Bai, Y. Photoelectron Spectroscopic Investigations of Porphyrins and Phthalocyanines on Ag (111) and Au (111): Adsorption and Reactivity. PhD thesis, Friedrich-Alexander-Universität Erlangen−Nürnberg, 2010.

(27) Pellegrino, G.; Condorelli, G. G.; Privitera, V.; Cafra, B.; Di Marco, S.; Alberti, A. Dye-Sensitizing of Self-Nanostructured Ti(:Zn)-O2/AZO Transparent Electrodes by Self-Assembly of 5,10,15,20-Tetrakis(4-carboxyphenyl)porphyrin. *J. Phys. Chem. C* **2011**, *115* (15), 7760−7767.

(28) Li, Z.; Berger, H.; Okamoto, K.; Zhang, Q.; Luscombe, C. K.; Cao, G.; Schlaf, R. Measurement of the Internal Orbital Alignment of Oligothiophene-TiO_2 Nanoparticle Hybrids. *J. Phys. Chem. C* **2013**, *117* (27), 13961−13970.

(29) Wiggins, B. C. Structural and Electronic Properties of Porphyrins and Phthalocyanines Self Assembled on Conductive Surfaces. Ph.D., Washington State University, Pullman, WA, 2013.

(30) Swadzba-Kwasny, M.; Chancelier, L.; Ng, S.; Manyar, H. G.; Hardacre, C.; Nockemann, P. Facile in Situ Synthesis of Nanofluids

DOI: 10.1021/acsami.6b10340
ACS Appl. Mater. Interfaces 2016, 8, 31403−31412

Based on Ionic Liquids and Copper Oxide Clusters and Nanoparticles. *Dalton Trans.* **2012**, *41* (1), 219−227.
(31) McIntyre, N. S.; Cook, M. G. X-ray Photoelectron Studies on Some Oxides and Hydroxides of Cobalt, Nickel, and Copper. *Anal. Chem.* **1975**, *47* (13), 2208−2213.
(32) Buchner, F.; Flechtner, K.; Bai, Y.; Zillner, E.; Kellner, I.; Steinrück, H.-P.; Marbach, H.; Gottfried, J. M. Coordination of Iron Atoms by Tetraphenylporphyrin Monolayers and Multilayers on Ag(111) and Formation of Iron-Tetraphenylporphyrin. *J. Phys. Chem. C* **2008**, *112* (39), 15458−15465.
(33) Karweik, D. H.; Winograd, N. Nitrogen Charge Distributions in Free-Base Porphyrins, Metalloporphyrins, and their Reduced Analogs Observed by X-ray Photoelectron Spectroscopy. *Inorg. Chem.* **1976**, *15* (10), 2336−2342.
(34) Bai, Y.; Sekita, M.; Schmid, M.; Bischof, T.; Steinruck, H.-P.; Gottfried, J. M. Interfacial Coordination Interactions Studied on Cobalt Octaethylporphyrin and Cobalt Tetraphenylporphyrin Monolayers on Au(111). *Phys. Chem. Chem. Phys.* **2010**, *12* (17), 4336−4344.
(35) Watcharinyanon, S.; Puglia, C.; Göthelid, E.; Bäckvall, J.-E.; Moons, E.; Johansson, L. S. O. Molecular Orientation of Thiol-Derivatized Tetraphenylporphyrin on Gold Studied by XPS and NEXAFS. *Surf. Sci.* **2009**, *603* (7), 1026−1033.
(36) Niwa, Y.; Kobayashi, H.; Tsuchiya, T. X-ray Photoelectron Spectroscopy of Tetraphenylporphin and Phthalocyanine. *J. Chem. Phys.* **1974**, *60* (3), 799−807.
(37) Gottfried, J. M.; Flechtner, K.; Kretschmann, A.; Lukasczyk, T.; Steinrück, H.-P. Direct Synthesis of a Metalloporphyrin Complex on a Surface. *J. Am. Chem. Soc.* **2006**, *128* (17), 5644−5645.
(38) Kretschmann, A.; Walz, M.-M.; Flechtner, K.; Steinruck, H.-P.; Gottfried, J. M. Tetraphenylporphyrin Picks up Zinc Atoms from a Silver Surface. *Chem. Commun.* **2007**, *6*, 568−570.
(39) Ghosh, A.; Fitzgerald, J.; Gassman, P. G.; Almlof, J. Electronic Distinction between Porphyrins and Tetraazaporphyrins. Insights from X-Ray Photoelectron Spectra of Free Base Porphyrin, Porphyrazine, and Phthalocyanine Ligands. *Inorg. Chem.* **1994**, *33* (26), 6057−6060.
(40) Zeller, M. V.; Hayes, R. G. X-ray Photoelectron Spectroscopic Studies on the Electronic Structures of Porphyrin and Phthalocyanine Compounds. *J. Am. Chem. Soc.* **1973**, *95* (12), 3855−3860.
(41) Beerbom, M. M.; Lägel, B.; Cascio, A. J.; Doran, B. V.; Schlaf, R. Direct Comparison of Photoemission Spectroscopy and in Situ Kelvin Probe Work Function Measurements on Indium Tin Oxide Films. *J. Electron Spectrosc. Relat. Phenom.* **2006**, *152* (1−2), 12−17.
(42) Schlaf, R.; Merritt, C. D.; Crisafulli, L. A.; Kafafi, Z. H. Organic Semiconductor Interfaces: Discrimination between Charging and Band Bending related Shifts in Frontier Orbital Line-up Measurements with Photoemission Spectroscopy. *J. Appl. Phys.* **1999**, *86* (10), 5678−5686.
(43) Coh, S. Electronic Structure and Binding Geometry of Tetraphenylporphyrin-Derived Molecules Adsorbed on Metal and Metal Oxide Surfaces. PhD thesis, Rutgers University Grad. School N. B., 2012.
(44) Koslowski, B.; Tschetschetkin, A.; Maurer, N.; Ziemann, P. 4-Mercaptopyridine on Au(111): a Scanning Tunneling Microscopy and Spectroscopy Study. *Phys. Chem. Chem. Phys.* **2011**, *13* (9), 4045−4050.

DOI: 10.1021/acsami.6b10340
ACS Appl. Mater. Interfaces 2016, 8, 31403−31412